*Stanford Exploration Project, Report 97, July 8, 1998, pages 45–60*

# Prestack Kirchhoff time migration for complex media

*Tariq Alkhalifah*[1]

***keywords:*** *time migration, anisotropy*


## ABSTRACT

Constructing the seismic image in vertical time, as opposed to depth, eliminates the inherent ambiguity of resolving the vertical $P$-wave velocity from surface seismic data in transversely isotropic media with a vertical axis of symmetry (VTI media). By ray tracing in the space-time ($x$-$\tau$)-domain, a traveltime map is built by interpolating the traveltime information along the rays onto a regular grid in space and time. This traveltime map is used by the prestack Kirchhoff time migration to obtain the migration summation trajectories. Since the traveltime map is extracted using ray tracing, the migration can practically handle any lateral velocity variations. Specifically, the prestack time migration yields good images of the isotropic and anisotropic Marmousi models.


## INTRODUCTION

Though the vertical axis of the earth subsurface is measured in units of distance, seismic images of the earth subsurface are usually presented in units of time. The process, referred to as time imaging, is practiced far more often than depth imaging. The reason for the preference of time imaging over the depth one is that we are simply unable to accuratly position reflecors in depth. Some researchers attribute this shortcoming to the presence of strong lateral inhomogeneity, but in areas of smooth velocity variations, the only proper explanation for the depth inaccuracies is the presence of anisotropy (Banik, 1984).

Time imaging algorithms, however, are based on the lateral homogeneity assumption, a condition that will restrict their use in areas of complex velocity structures. As a result, depth migration is used in these regions despite the inherent ambiguity of estimating depth from surface seismic data. In transversely isotropic media with vertical symmetry axis (VTI media), this implies that we need to estimate the vertical velocity in order to do depth migration. However, the vertical velocity cannot be estimated from surface seismic data. More information is needed to estimate the

[1]**email:** tariq@sep.stanford.edu

vertical velocity (i.e., well log or check shot data).

Alkhalifah et al. (1997) derived an eikonal and ray tracing equations for VTI media in the ($x$-$\tau$)-domain. These equations are slightly more complicated than their depth counterparts, yet they can be solved as efficiently using standard numerical methods. Alkhalifah et al. (1997) also show that these traveltime equations are some-what independent of the vertical velocity in VTI media. Instead, these equations depend on two parameters: the NMO velocity for a horizontal reflector and the anisotropy parameter, referred to as $\eta$. Conveniently, these two parameters can be estimated from surface seismic $P$-wave data (Alkhalifah and Tsvankin, 1995).

In this paper, I use Alkhalifah et al. (1997) traveltime equations, specifically the ray tracing ones, to build traveltime tables in the ($x$-$\tau$)-domain. These traveltime tables are subsequently used to implement prestack Kirchhoff time migration. The accuracy of the migration is demonstrated on the isotropic, as well as the anisotropic, Marmousi dataset.

## REPRESENTING DEPTH WITH VERTICAL TIME

In this section, I will summarize the derivation of the VTI eikonal equation for the ($x$-$\tau$)-domain, derived originally by Alkhalifah et al. (1997).

Obviously, the two-way vertical traveltime is related to depth,

$$\tau(x,z) = \int_0^z \frac{2}{v_v(x,\zeta)} d\zeta, \tag{1}$$

where $v_v$ is the vertical $P$-wave velocity, which can vary vertically as well as laterally. As a result, the stretch applied to the depth axis is laterally variant.

Alkhalifah (1997a) derived a simple form of the eikonal equation for VTI media, based on setting the shear wave velocity to zero. For 2-D media, it is

$$\begin{aligned} v^2\,(1+2\,\eta)\left(\frac{\partial t}{\partial x}\right)^2 - {v_v}^2\left(\frac{\partial t}{\partial z}\right)^2 & \\ \left(1-2\,v^2\,\eta\left(\frac{\partial t}{\partial x}\right)^2\right) &= 1. \end{aligned} \tag{2}$$

This equation, based on the acoustic medium assumption in VTI media, though not physically possible, yields extremely accurate traveltime solutions that are close to what we find for typical elastic media.

Clearly, equation 2 includes first-order derivatives of traveltime with respect to position. In order to transform this eikonal equation from depth to time, we need to replace $x$ with $\tilde{x}$, as well. Using the chain rule, $\frac{\partial t}{\partial x}$ in the eikonal equation 2 is given by

$$\frac{\partial t}{\partial x} = \frac{\partial t}{\partial \tilde{x}} + \frac{\partial t}{\partial \tau}\sigma, \tag{3}$$

where $\sigma$, derived from equation (1),

$$\sigma(x,z) = \frac{\partial \tau}{\partial x} = \int_0^z \frac{\partial}{\partial x}\left(\frac{1}{v_v(x,\zeta)}\right)\, d\zeta. \tag{4}$$

Likewise, the partial derivative in $z$ of the eikonal equation is

$$\frac{\partial t}{\partial z} = \frac{2}{v_v}\frac{\partial t}{\partial \tau}. \tag{5}$$

Therefore, the transformation from $(x,\ z)$ to $(\tilde{x},\ \tau)$ is governed by the following Jacobian matrix in 2-D media:

$$J = \begin{pmatrix} 1 & \sigma \\ 0 & \frac{2}{v_v} \end{pmatrix} \tag{6}$$

Substituting equations (3) and (5) into the eikonal equation (2) yields an eikonal equation in the $(x - \tau)$-domain given by

$$v^2\ (1+2\,\eta)\left(\frac{\partial t}{\partial \tilde{x}} + \frac{\partial t}{\partial \tau}\sigma\right)^2 - 4\left(\frac{\partial t}{\partial \tau}\right)^2 \left(1 - 2\,v^2\,\eta\left(\frac{\partial t}{\partial \tilde{x}} + \frac{\partial t}{\partial \tau}\sigma\right)^2\right) = 1, \tag{7}$$

which is also indirectly independent on the vertical velocity. However, according to equation (4), $\sigma$ still depends on the vertical $P$-wave velocity. Alkhalifah et al. (1997) demonstrated that if the medium was factorized laterally ($v_v(x,z) = \alpha(z)v(x,z)$), then

$$\sigma(\tilde{x},\tau) = \frac{-1}{v(\tilde{x},\tau)}\int_0^\tau \frac{\partial v(\tilde{x},\tilde{\tau})}{\partial \tilde{x}}\, d\tilde{\tau}. \tag{8}$$

which is independent of the vertical velocity. The departure of the medium from this special condition of laterally factorized media will cause errors in traveltime calculation; these errors, however, are generally small.

Using the method of characteristics, Alkhalifah et al. (1997) derived a system of ordinary differential equations that define the ray trajectories in the $(x - \tau)$-domain. Numerical solutions of the raytracing equations, as opposed to the eikonal equation, provide multi-arrival traveltimes and amplitudes, a feature that is key to properly image the Marmousi model (Geoltrain and Brac, 1993). Thus, in the Kirchhoff migration examples, I use $(x - \tau)$-domain traveltime maps extracted from ray tracing.

## THE MARMOUSI MODEL

The Marmousi data set was generated at the Institute Francais du Petrole (IFP), and was used for the workshop on practical aspects of seismic data inversion at the 1990 EAEG meeting in Copenhagen, where different groups (contractors, universities, and oil companies) applied their proffered imaging tools on this data set. Detailed accounting of what transpired at the workshop is given by Versteeg and Grau (1990) and Versteeg and Lailly (1991). The original Marmousi data set is generated using a 2-D acoustic finite-difference modeling program.

One of the biggest contributions of the Marmousi model is that it demonstrated the limitations of first-arrival traveltimes in imaging complex media. Specifically, Geoltrain and Brac (1993) showed that to properly image the Marmousi model we need multi-arrival traveltimes. In portions of the Marmousi model, or any other complex model, the first arrival is not necessarily the most energetic. Therefore, reflected energy from key horizons, such as the top of the reservoir, are not properly imaged by using only first arrival traveltimes.

The original Marmousi model was built to resemble an overall continental drift geological setting. Numerous large normal faults were created as a result of this drift. The geometry of the Marmousi is based somewhat on a profile of the North Quenguela through the Cuanza basin (Versteeg, 1993). The target zone is a reservoir located at a depth of about 2500 m. The model contains many reflectors, steep dips, and strong velocity variations in both the lateral and the vertical direction (with a minimum velocity of 1500 m/s and a maximum of 5500 m/s).

Figure 1 shows a smoothed version of the Marmousi model displayed in the $(x-z)$-domain (top) and the $(x-\tau)$-domain (bottom). The smoothing operator, a 100 m box car function in 2-D, was applied in the $(x-z)$-domain. This same velocity is used to convert the depth axis to a time one using equation (1). The time section seems more complicated than the depth one, because the velocity-based depth conversion increased the apparent folding of the velocity model. Nevertheless, the output of raytracing using this new velocity model should be equivalent to the output of the conventional ray tracing using the depth velocity model.

In my paper from last fall (Alkhalifah, 1997a), I generated an anisotropic Marmousi dataset in a similar manner in which the isotropic one was generated (finite difference). I used exactly the same geometry settings used in building the the original isotropic dataset. Thus, all the parameter settings needed to perform migration on the isotropic Marmousi dataset can be used for the anisotropic one as well. The NMO and vertical velocity of the anisotropic model are the same as for the original Marmousi velocity model provided by IFP. The $\eta$ model, shown in Figure 2, has overall the same characteristics as the velocity model. It too has to be converted to time before usage in the migration.

## TRAVELTIME MAPS

To implement prestack Kirchhoff migration, we need first to construct traveltime maps (the Greens function) used to define the migration summation trajectories. Ray tracing is used for this task, and in particular $(x-\tau)$-domain ray tracing. However, ray tracing only provides traveltime information along the ray paths. As a result, cubic interpolation is used to place the traveltime information on a regular grid.

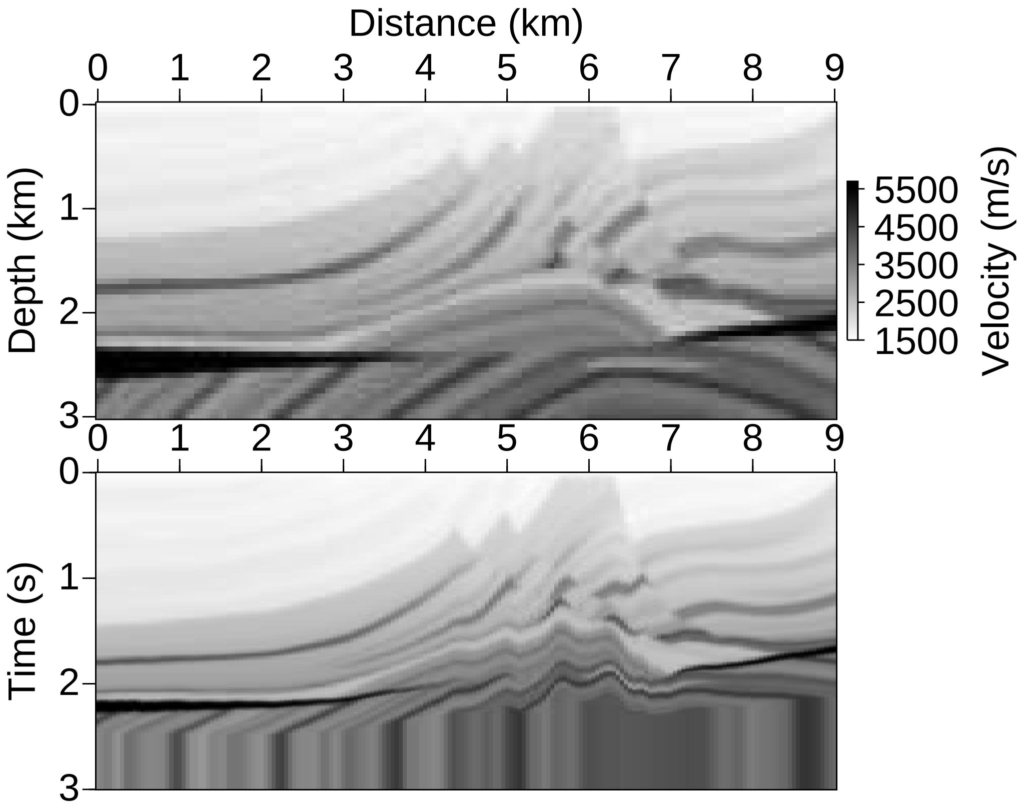


Figure 1: A smoothed version of the Marmousi velocity model displayed with the vertical axis given in depth (top) and in time (bottom). The smoothing operator consisted of a 2-D box car function with a 100 m length in each dimension. tariq4-vel [NR]

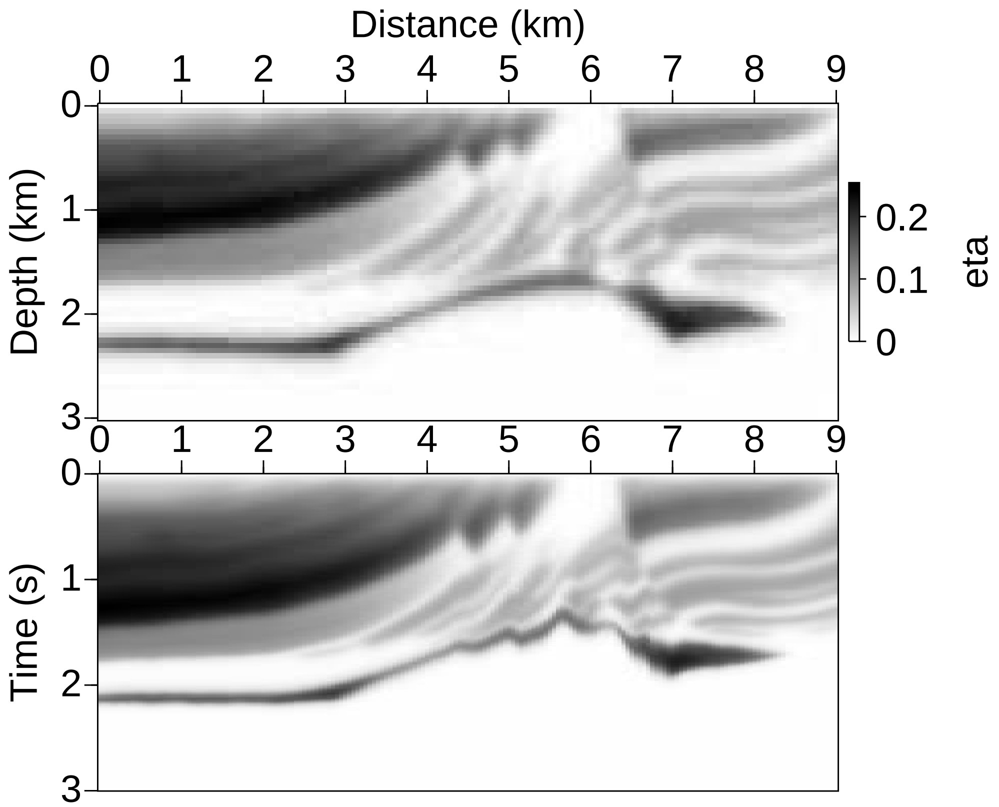


Figure 2: A smoothed version of the $\eta$ model displayed with the vertical axis given in depth (top) and in time (bottom). The smoothing operator consisted of a 2-D box car function with a 200 m length in each dimension. tariq4-eta [NR]

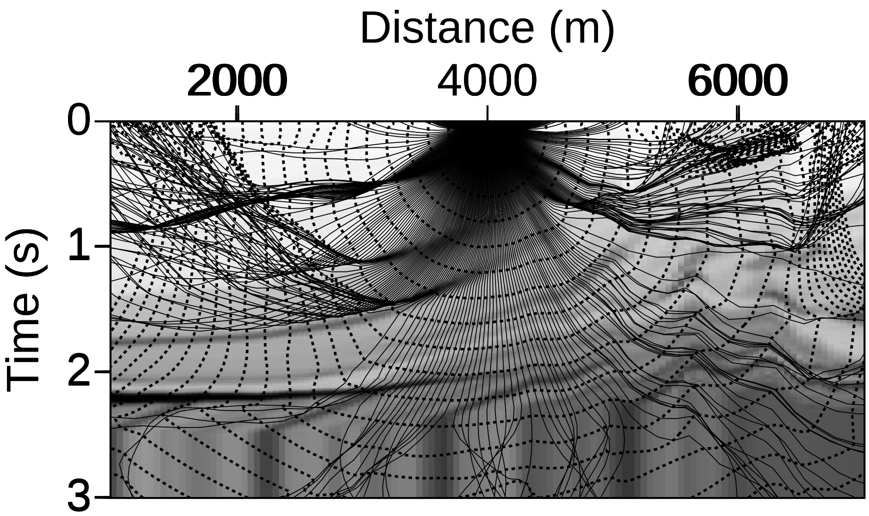


Figure 3: Rays (solid lines) and wavefront (dashed lines) calculated using the $(x-\tau)$-domain ray tracing for waves emanating from a source at surface location 4000 m. In the background the smooth version of the Marmousi velocity model used for the traveltime calculation is displayed. $\boxed{\text{tariq4-vel-time-ray4000}}$ [NR]

Figure 3 shows rays emanating from a source at a surface location 4000 m. Traveltime along these rays are used to create a traveltime map with time values given by the dashed contour curves. These dashed curves, thus represent the wavefronts of the propagating waves. In $(x - \tau)$-domain, the wavefronts do not necessarily have to be perpendicular to the rays, even for isotropic media. Faster wavefronts are in agreement with high velocity zones, displayed in background. Clearly, from Figure 3 we can see regions of minimal ray coverage, which makes the task of interpolating of the traveltime information to these regions a little more ambiguous. However, such regions also have low energy and thus contribute little to the image. These areas of low ray coverage exist mainly in areas surrounded by cusps. For the purpose of migration, traveltime information in regions of large lateral distance from the source, compared to depth (or vertical time in this case), are often discarded. This typically includes the area directly under surface location 6000 m, which seemingly has suspect traveltime contours.

Traveltimes can also be calculated directly from finite difference solution of the eikonal equation. Specifically, I use the fast marching method in polar coordinates (Alkhalifah and Fomel, 1997) to generate traveltimes in the $(x - z)$-domain. To compare these traveltimes with the ones obtained from $(x - \tau)$-domain raytracing, I convert the raytracing traveltime maps from time to depth. Figure 4 shows contour

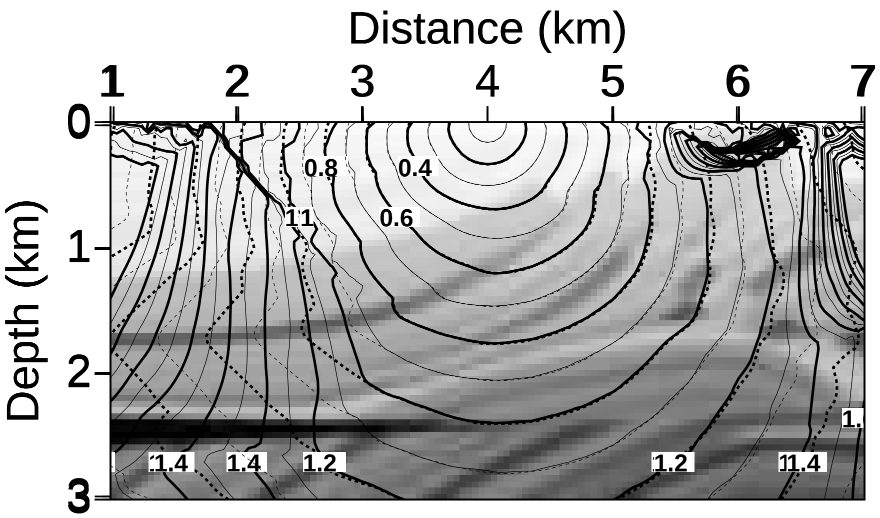


Figure 4: Contours of traveltime plotted in depth calculated using $(x - \tau)$-domain ray tracing followed by a time-to-depth conversion (solid lines), and the eikonal solver (dashed curve), again for waves emanating from a source at surface location 4000 m. The smoothed Marmousi model is again displayed in the background. $\boxed{\text{tariq4-time-cont4000}}$ [NR]

lines from both traveltime maps, with the velocity field displayed in the background. Clearly, the traveltime contours obtained using $(x-\tau)$-domain raytracing agree well with those obtained via the eikonal solver in areas around the source. Differences occur in areas dominated by traveltime triplications, as can be deduced from Figure 3. The finite difference solution of the eikonal equation provides only the fastest energy solution, not necessarily the most useful (energetic), while the raytracing equations are capable of producing all ray-theoretical solutions, and thus one can choose the most energetic solution.

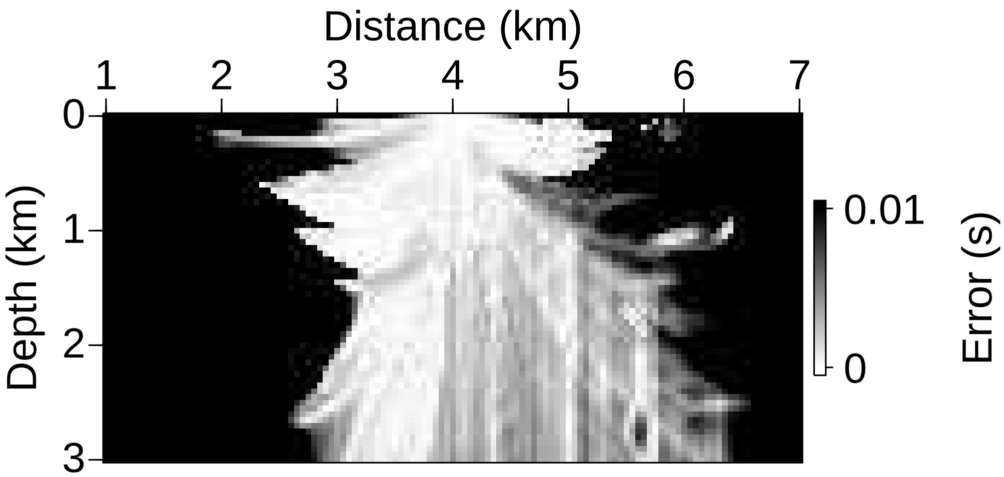


Figure 5: The absolute difference between the two traveltime maps shown in Figure 4. This image is clipped at a maximum error of 10 ms. tariq4-error4000 [NR]

The absolute difference between the two traveltime maps is shown in Figure 5. Errors of 10 ms and beyond are given the color black. The areas of clear differences between the two traveltime solutions coincide with areas of multi-arrival traveltimes (triplications), as can be seen in Figure 3. The eikonal solution provides the fastest arrival; ray tracing via interpolation, provides the most energetic solution.

## PRESTACK MIGRATION OF THE MARMOUSI DATASET

Due to the complexity of the velocity model, depth migration is often used to properly prestack migrate the Marmousi dataset. Time migration typically yields poor images of the Marmousi model. However, using the traveltime maps obtained from the $(x-\tau)$-domain ray tracing, good images of the Marmousi model are possible in time.

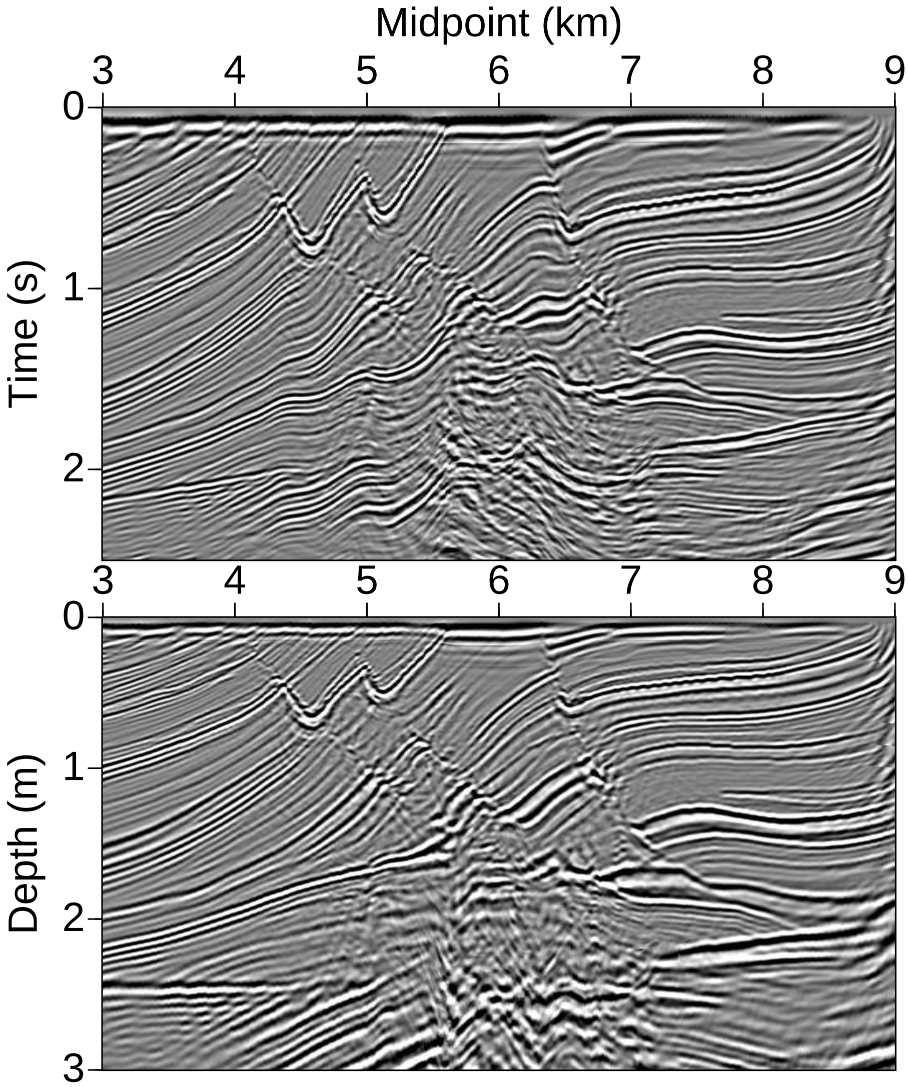


Figure 6: Stacked sections after prestack time imaging given in time (top), and converted to depth (bottom). The time-to-depth conversion is applied using the smoothed Marmousi velocity field. tariq4-mig [NR]

Figure 6 (top) shows stacked section after prestack time-migration. Overall, the migrated section seems well focused, and since the vertical axis is given in time, the position of the reflectors is affected by the velocity model. The reflectors appear more shaky under areas of complex velocity structure. The conversion of this data from time to depth will remove such artificial complexity. Figure 7 shows common CMP gathers after prestack time migration. Stacking such gathers produces for us the image shown in Figure 6 (top). At all times, the moveout is well aligned, ready to be stacked. Some misalignment appears at CMP location 5000 and 6000 m, but this is expected considering the complexity of the Marmousi Model. The confirmation of the accuracy of the migration will allow its use for velocity estimation, since non-alignment of the moveout cannot be blamed on the migration, and will be only attributed to velocity inaccuracies.

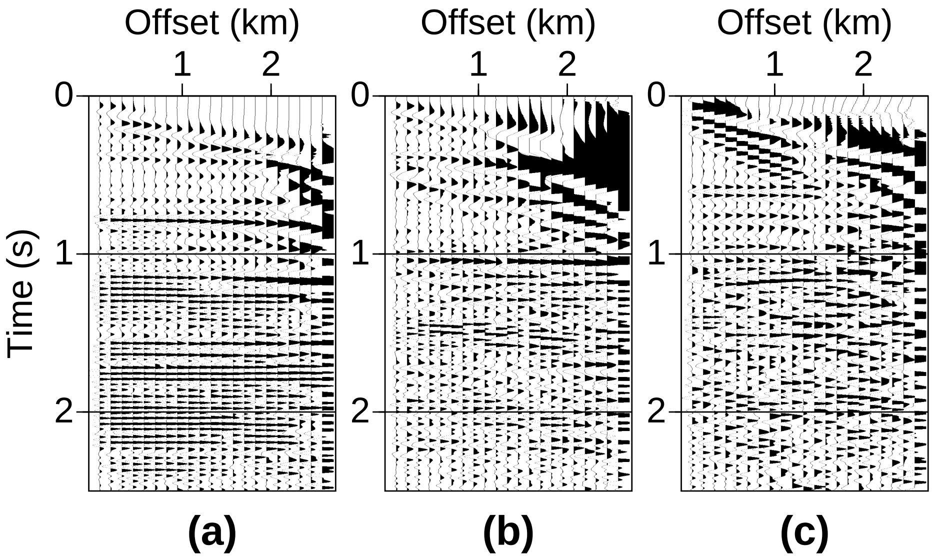


Figure 7: Common CMP gathers after prestack time migration for CMP locations (a) 4000 m, (b) 5000 m, and (c) 6000 m. These gathers, and other ones, are stacked to give us the section in Figure 6 (top). tariq4-iscmp [NR]

Figure 6 (bottom) shows the stacked section after prestack time migration, but in depth rather than time. Using the Marmousi velocity model for the conversion has rendered more accurate reflector positioning than that in the time domain. In imaging the reservoir anticline, some fault-like breaks appeared in the depth image. This can be attributed to the complexity of the model directly above this region, which might have negatively affected the time-to-depth conversion. For prestack migration velocity analysis we have yet to see which domain (depth or time) will result in better convergence and stability. However, some preliminary indications favor the time domain (Biondi et al., 1997), simply because horizontal reflectors are nearly stationary in such a domain, and moveout from horizontal reflectors provides the majority of the velocity information in the subsurface.

## ANISOTROPIC PRESTACK MIGRATION

To apply prestack VTI migration in the $(x-\tau)$-domain, we will need the NMO velocity field as well as $\eta$. Using a smoothed version of both fields, shown above, I prestack migrate the anisotropic Marmousi dataset in the same way I did the isotropic one. However, we must first compute the traveltime map using the ray tracing equations of Alkhalifah et al. (1997), which hold for VTI media as well.

Figure 8 shows rays emanating from a source at surface position of 4000 m. The traveltime information along the rays are interpolated to a regular grid in the same way as the isotropic case. The contours in Figure 8 show traveltimes corresponding to the interpolated Field. The rays and traveltimes are different from the isotropic ones, shown in Figure 3, especially for large ray angles. Figure 9 (top) shows, again,

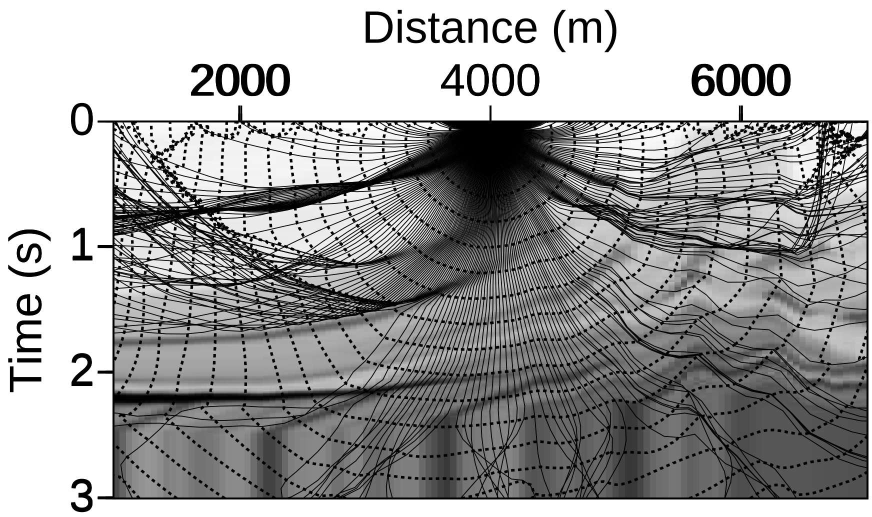


Figure 8: Rays (solid lines) and wavefront (dashed lines) calculated using the $(x-\tau)$-domain ray tracing for waves emanating from a source at surface location 4000 m. In the background the smooth version of the Marmousi velocity model used for the traveltime calculation is displayed. The medium here is VTI with $\eta$ given by Figure 2. tariq4-vel-time-ray4000ti [NR]

a stacked section after prestack time-migrated, but for the anisotropic Marmousi dataset. Overall, the migrated section seems well focused, better focused than the isotropic result. This is because the anisotropic dataset, which is new, has slightly

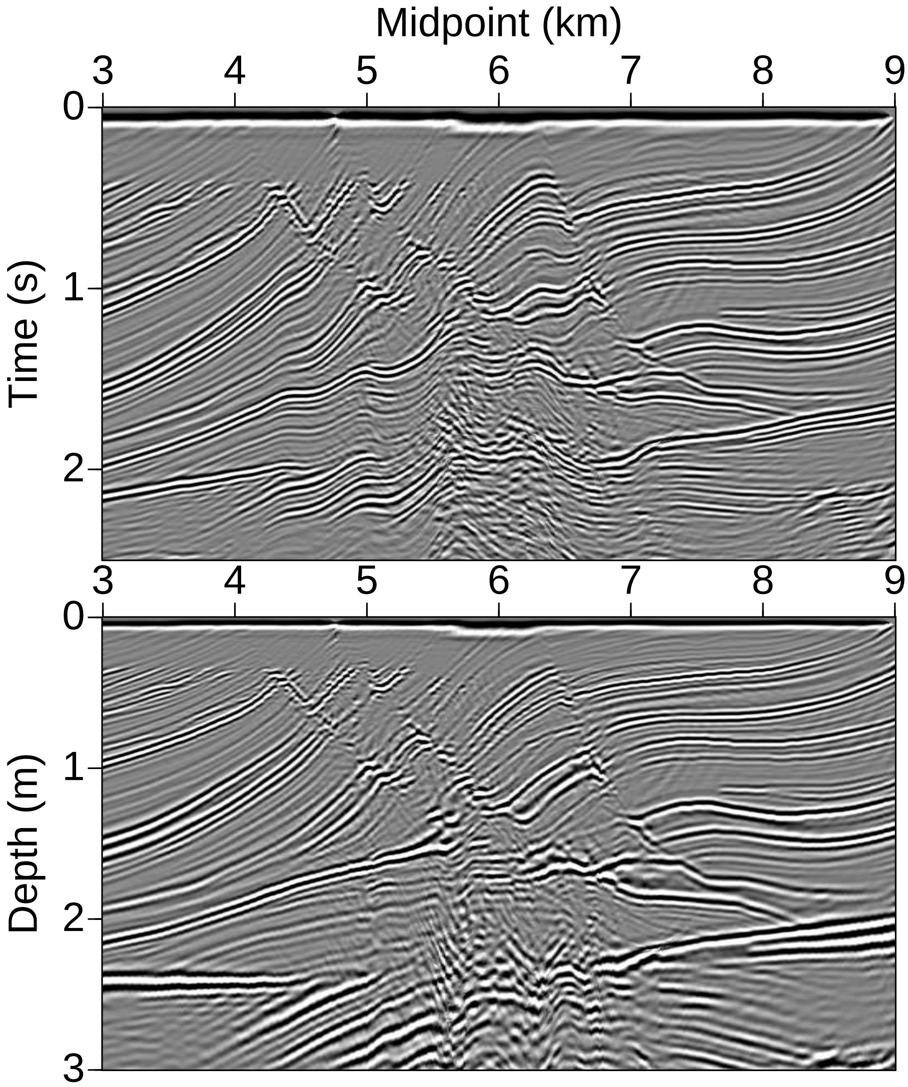


Figure 9: Stacked sections after prestack anisotropic time imaging given in time (top), and converted to depth (bottom). The time-to-depth conversion is applied using the smoothed Marmousi velocity field. $\boxed{\text{tariq4-migti}}$ [NR]

higher peak frequencies and a better, less vibrating, source. Figure 10 shows common CMP gathers after prestack anisotropic time migration. Despite the large nonhyperbolic moveout that often accompany reflections in VTI media (see Alkhalifah (1997a)), the moveout is well aligned here. These outstanding alignments hold for the complex, as well as the smooth, regions of the model.

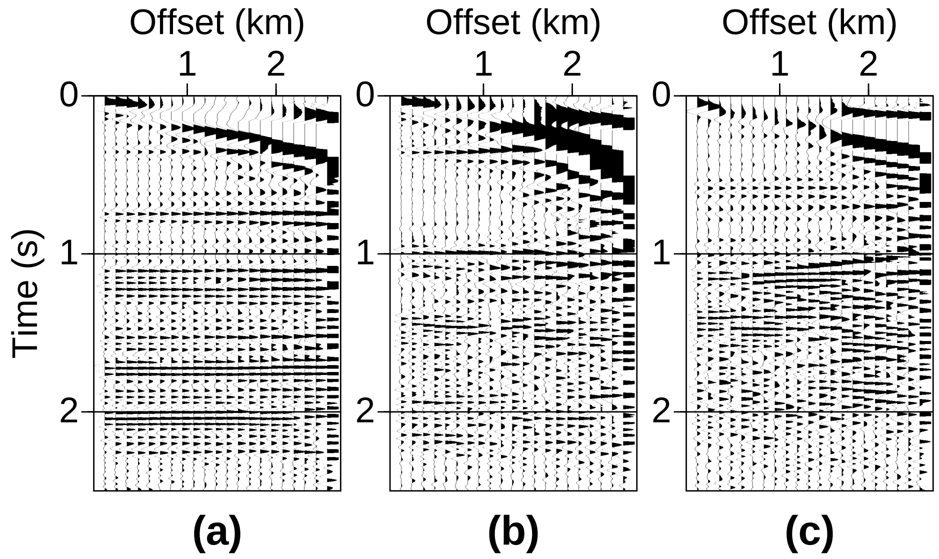


Figure 10: Common CMP gathers after prestack anisotropic time migration for CMP locations (a) 4000 m, (b) 5000 m, and (c) 6000 m. These gathers, and other ones, are stacked to give us the section in Figure 9 (top). tariq4-ticmp [NR]

Finally, Figure 6 (bottom) shows the stacked section after prestack anisotropic time migration in depth. Here, I use the same velocity model used in the isotropic case for the conversion from time to depth, since this velocity also represents the vertical velocity. In practical applications, we would need to use a vertical velocity model built from information extracted from the available wells in the area, since the surface $P$-wave seismic data do not hold any explicit information about the vertical velocity. The time migration, in its original intension, allowed us to delay the depth representation of the seismic image to whenever such depth information becomes available. Yet, using this time migration, we managed to image and focus data as complex as the Marmousi model. This feature is particularly important in prestack-based parameter estimation.

## CONCLUSIONS

Prestack time migrating the Marmousi model seems like an ingredient for disaster, especially since the Marmousi model is complex and time migration conventionally does not handle complex media. However, a ray-tracing based time migration can handle any lateral inhomogeneity and is only guided by the limitations of ray theory. Using such an $(x - \tau)$-domain ray tracing, good images of the Marmousi model are obtained. In VTI media, this time migration allows us to avoid estimating the vertical velocity, a parameter that is typically not resolvable from surface seismic data.

## ACKNOWLEDGMENTS

I thank Biondo Biondi and Sergey Fomel for the many useful discussions we had on this subject.

## REFERENCES

Alkhalifah, T., and Fomel, S., 1997, Implementing the fast marching eikonal solver: Spherical versus cartesian coordinates: SEP–**95**, 149–171.

Alkhalifah, T., and Tsvankin, I., 1995, Velocity analysis for transversely isotropic media: Geophysics, **60**, 1550–1566.

Alkhalifah, T., Fomel, S., and Biondi, B., 1997, Time-domain anisotropic processing in arbitrarily inhomogeneous media: SEP–**95**, 77–99.

Alkhalifah, T., 1997a, An acoustic wave equation for anisotropic media: SEP–**95**, 283–307.

Alkhalifah, T., 1997b, An anisotropic Marmousi model: SEP–**95**, 265–282.

Banik, N. C., 1984, Velocity anisotropy of shales and depth estimation in the north sea basin: Geophysics, **49**, no. 9, 1411–1419.

Biondi, B., Fomel, S., and Alkhalifah, T., 1997, "focusing" eikonal equation and global tomography: SEP–**95**, 61–76.

Geoltrain, S., and Brac, J., 1993, Can we image complex structures with first-arrival traveltime?: Geophysics, **58**, no. 4, 564–575.

Versteeg, R., and Grau, G., 1990, Practical aspects of seismic data inversion, the Marmousi experience Practical aspects of seismic data inversion, the Marmousi experience, Eur. Assoc. Expl. Geophys., Proceedings of 1990 EAEG Workshop, 52nd EAEG Meeting, 1–194.

Versteeg, R., and Lailly, P., 1991, Eaeg workshop report: Practical aspects of seismic data inversion: First Break, **9**, no. 2, 75–80.

Versteeg, R. J., 1993, Sensitivity of prestack depth migration to the velocity model: Geophysics, **58**, no. 6, 873–882.